Supplementary Information

0D ultrafine ruthenium quantum dots decorated 3D porous graphitic carbon nitride with efficient charge separation and appropriate hydrogen adsorption capacity for superior photocatalytic hydrogen evolution

Pengfei An, Weihao Zhu, Luying Qiao, Shichao Sun, Yuyan Xu, Deli Jiang, Min Chen*, and Suci Meng*

School of Chemistry and Chemical Engineering, Jiangsu University, Xuefu Road 301, Zhenjiang 212013, China

Corresponding author: Min Chen, Suci Meng

E-mail address:

chenmin3226@sina.com (M. Chen);

mengsc@ujs.edu.cn (S. C. Meng)

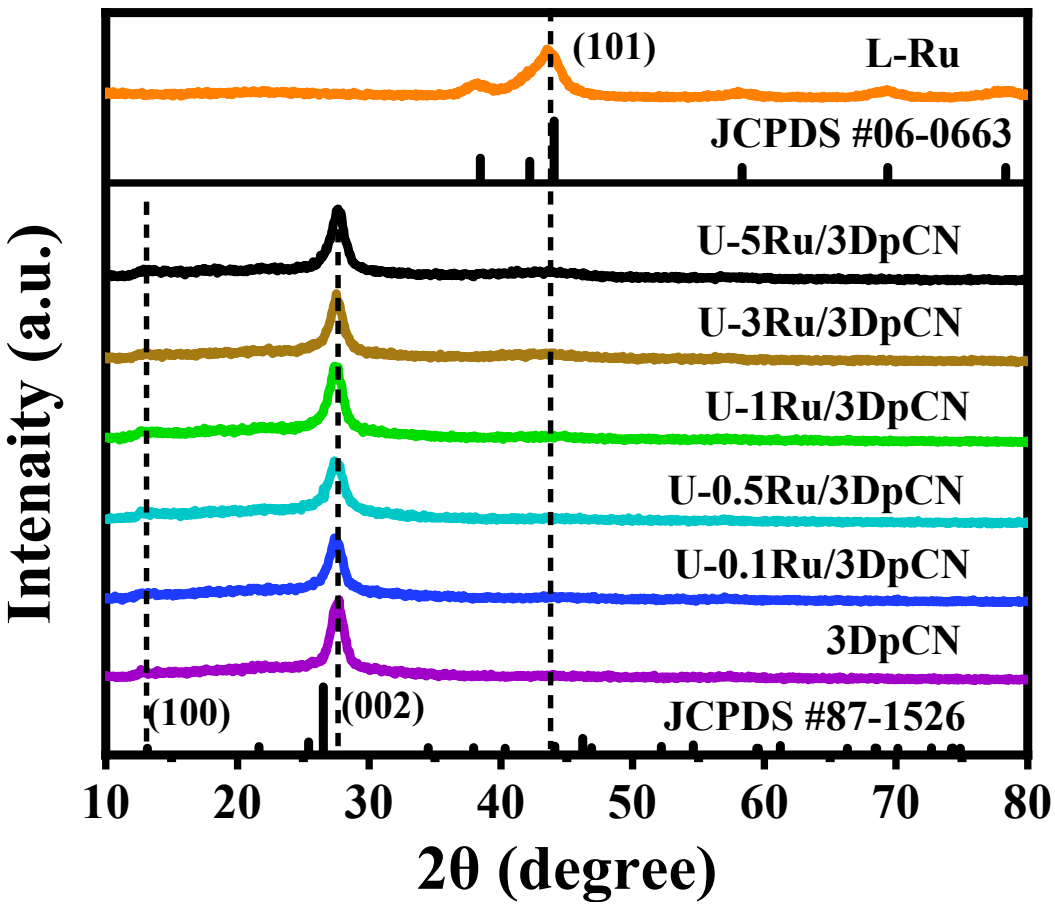

Figure S1. XRD patterns of L-Ru, 3DpCN, and U-Ru/3DpCN composites with different Ru loading ratios.

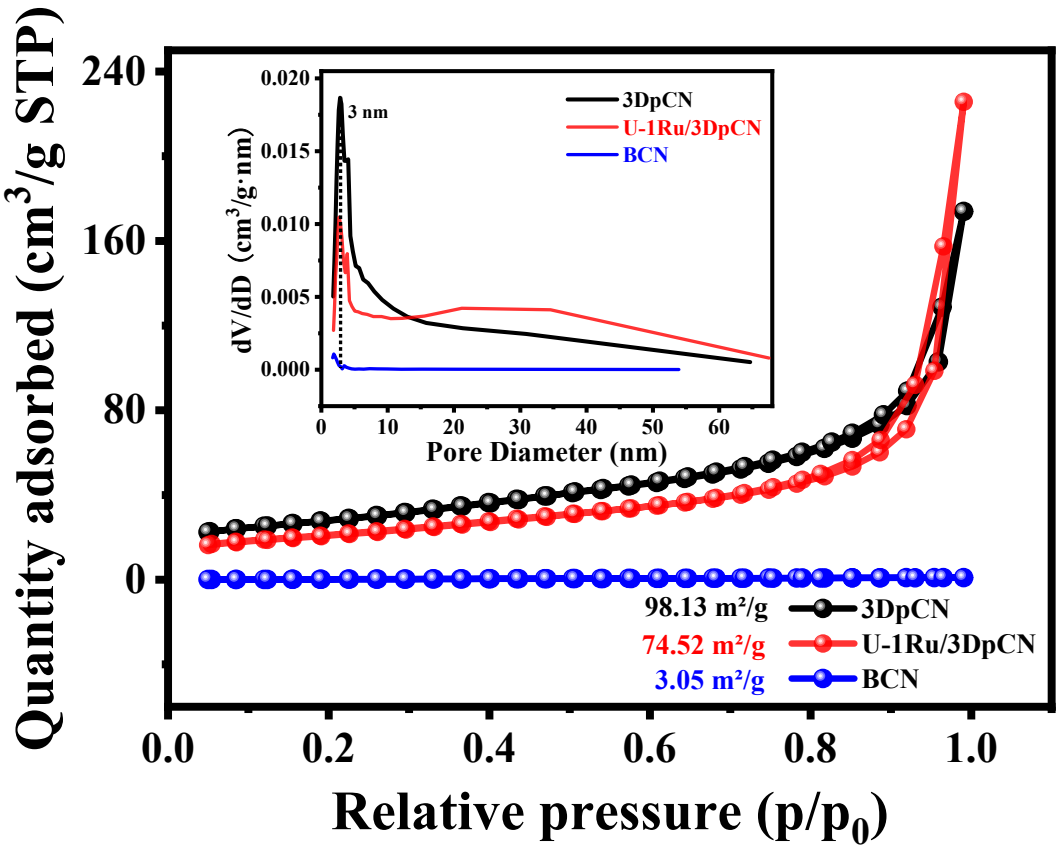

Figure S2. N_2 adsorption-desorption isotherms and BJH pore size distribution plots (inset) of the BCN, 3DpCN, and U-1Ru/3DpCN.

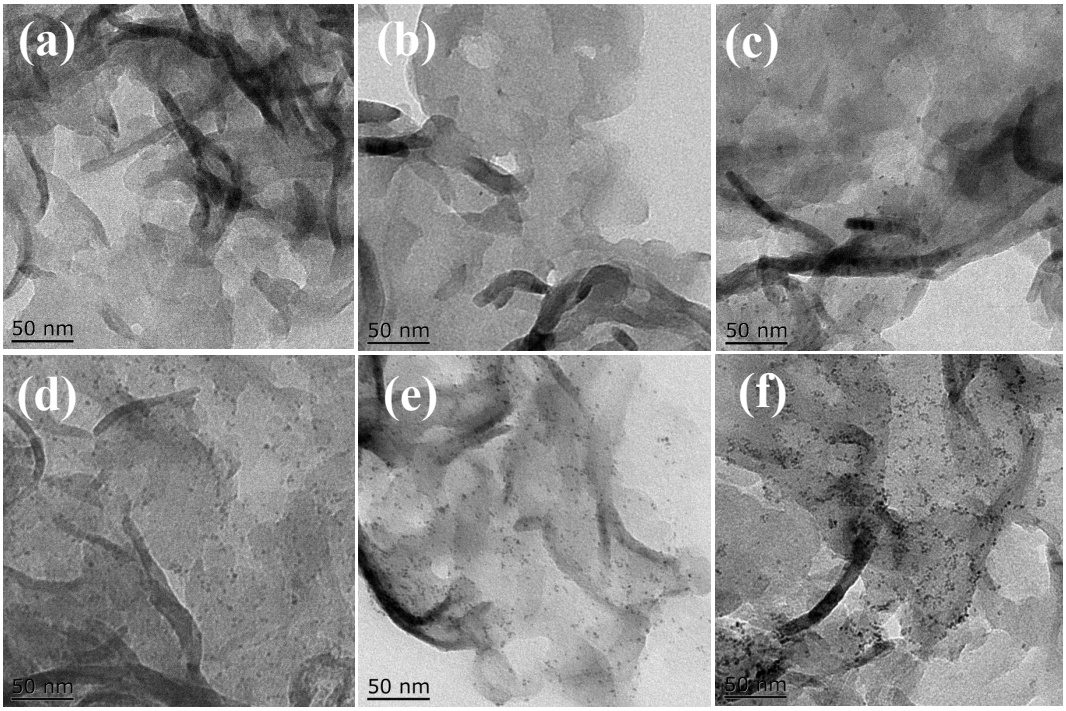

Figure S3. TEM images of (a) 3DpCN, (b) U-0.1Ru/3DpCN, (c) U-0.5Ru/3DpCN, (d) U-1Ru/3DpCN, (e) U-3Ru/3DpCN, and (f) U-5Ru/3DpCN.

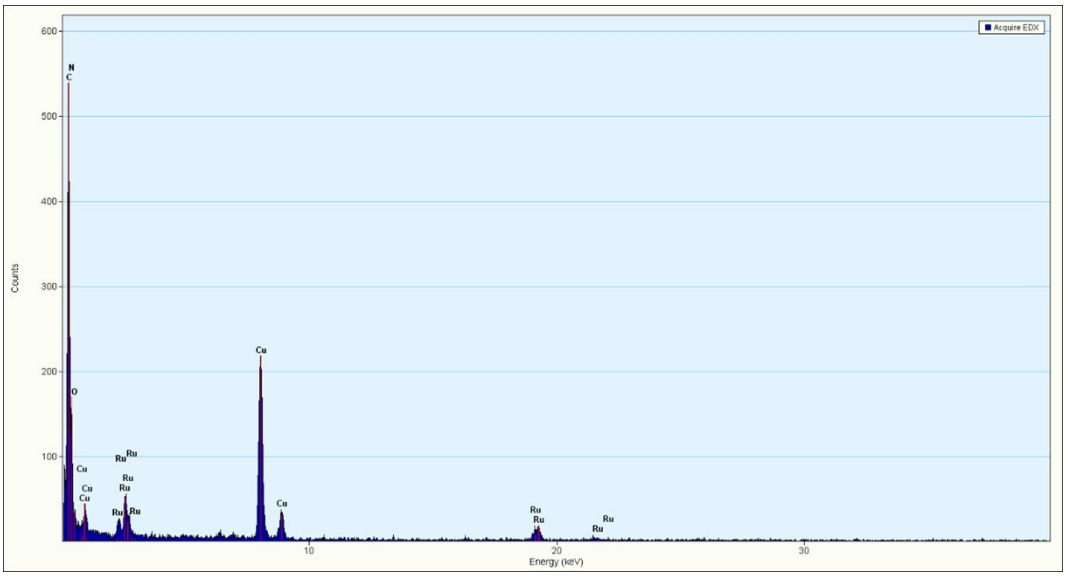

Figure S4. EDX spectrum of U-1Ru/3DpCN.

Figure S5. Physical appearance of (a) 3DpCN, (b)U-0.1Ru/3DpCN, (c) U-0.5Ru/3DpCN, (d) U-1Ru/3DpCN, (e) U-3Ru/3DpCN, and (f) U-5Ru/3DpCN.

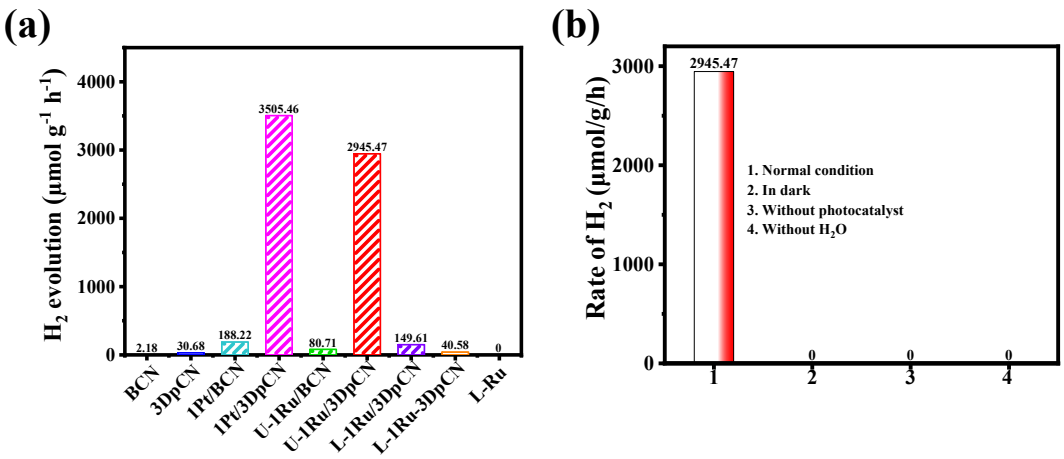

Figure S6. (a) comparison of the average hydrogen evolution rate of as-prepared photocatalysts under 5 h visible light irradiation; (b) photocatalytic hydrogen evolution performance under various conditions.

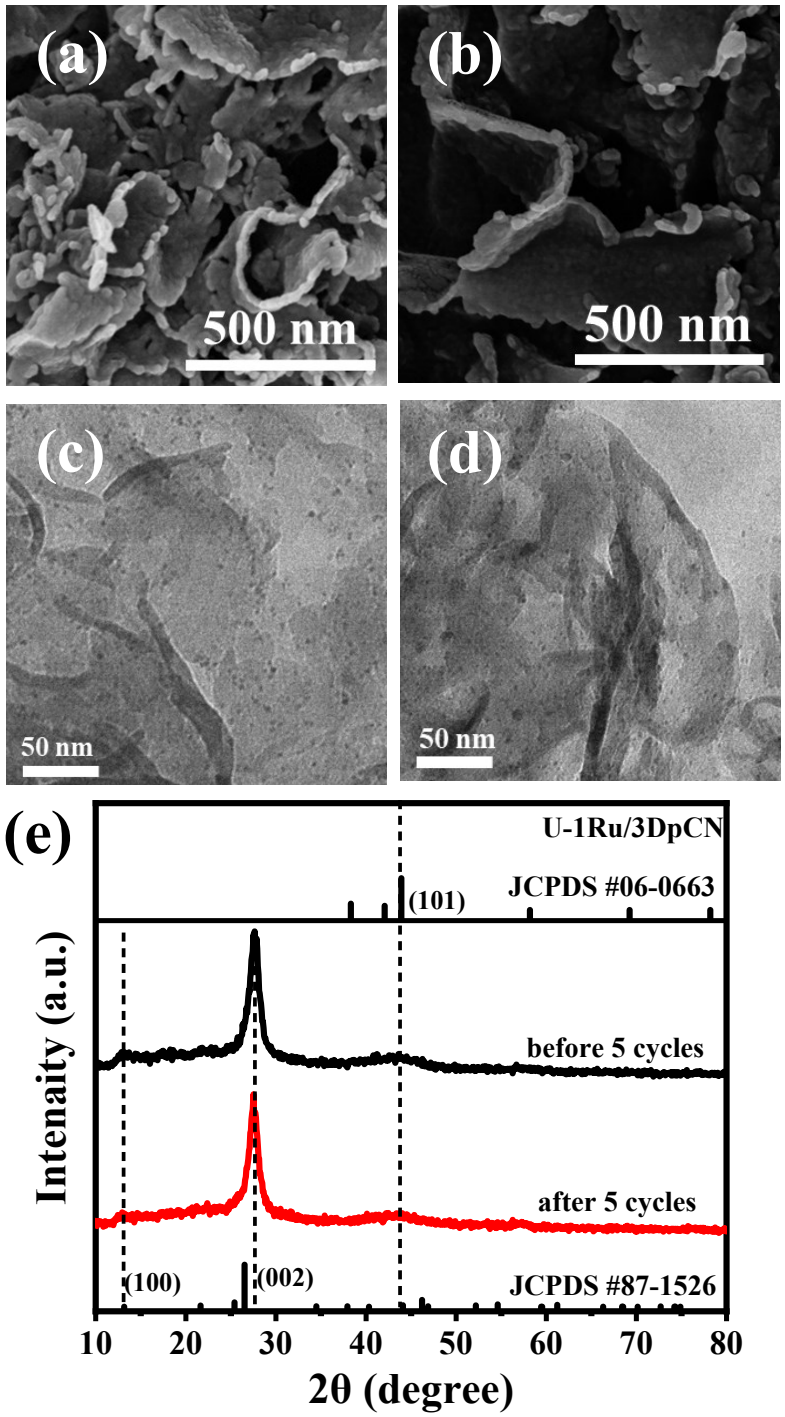

Figure S7. SEM images of U-1Ru/3DpCN (a) before and (b) after 5 cycles; TEM images of U-1Ru/3DpCN (c) before and (d) after 5 cycles; and (e) XRD patterns of U-1Ru/3DpCN before and after 5 cycles.

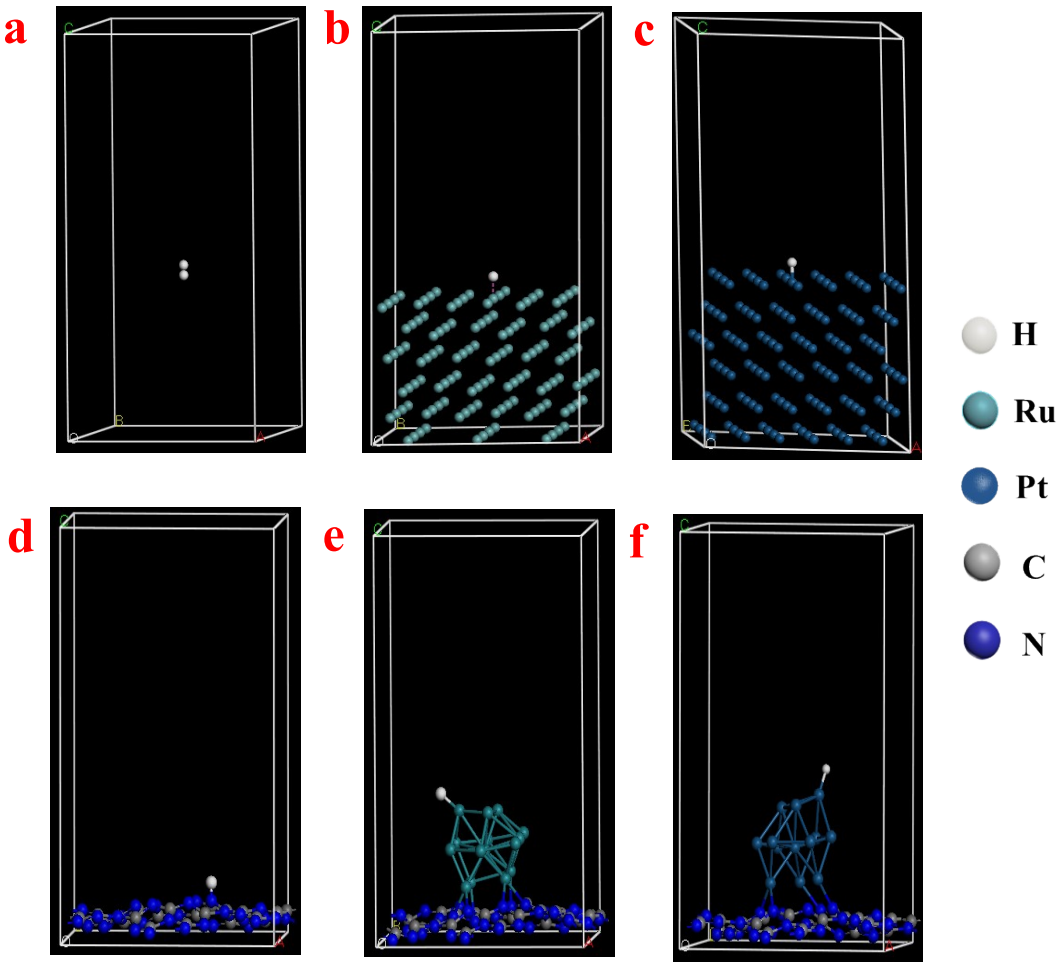

Figure S8. (a) H_2 model and H* adsorption models on the surface of (b) Ru (101), (c) Pt (111), (d) g-C_3N_4, (e) Ru (101)/g-C_3N_4, and (f) Pt (111)/g-C_3N_4.

Table S1. Element contents in U-1Ru/3DpCN

	Ru		C		N		Ru: C
Characterizations	Weight %	Atomic %	Weight %	Atomic %	Weight %	Atomic %	Mol ratio
EDX (part)	2.69	0.36	38.01	57.03	59.31	42.62	0.0086: 1
XPS (surface)	/	0.34	/	37.86	/	59.63	0.0090 :1

Exponential decay-fitted parameters of fluorescence lifetime：

The TRPL decay signals can be fitted by single/dual-exponential decay kinetics function, and usually adopt the dual-exponential decay kinetics function to fit TRPL decay signal, just as displayed in manuscript:

$$I(t) = A_1 \cdot \exp(-t/\tau_1) + A_2 \cdot \exp(-t/\tau_2)$$

As shown in **Table S2**, τ_1 and τ_2 were obtained by the equation: $y = y_0 + A_1*\exp(-x/\tau_1) + A_2*\exp(-x/\tau_2)$ rather than man-made. And the average emission lifetime of the emission decay can be also calculated through the following equation:

$$\tau = \frac{A_1 \cdot \tau_1^2 + A_2 \cdot \tau_2^2}{A_1 \cdot \tau_1 + A_2 \cdot \tau_2}$$

where τ_1 represents the fluorescence decay time of the excited electrons from the conduction band (CB) to the valence band (VB) of g-C_3N_4, τ_2 is the fluorescence decay time of the recombination of photo-generated electron-hole pairs on the surface of g-C_3N_4, and A_1 and A_2 are the relative intensities.

Table S2. Calculation details of TRPL.

Model	ExpDecay 2	
Equation 1	$y = y_0 + A_1*\exp(-(x-x_0)/\tau_1) + A_2*\exp(-(x-x_0)/\tau_2)$	
Equation 2	$\tau = \frac{A_1 \bullet \tau_1^2 + A_2 \bullet \tau_2^2}{A_1 \bullet \tau_1 + A_2 \bullet \tau_2}$	
Sample	3DpCN	U-1Ru/3DpCN
$\mathbf{Y_0}$	0. 03189	0. 0348
$\mathbf{X_0}$	125. 66005	125. 57553
$\mathbf{A_1}$	0. 75215	0. 19362
$\boldsymbol{\tau_1}$**/ns**	0. 34607	0. 11895
$\mathbf{A_2}$	0.3086	0. 71656
$\boldsymbol{\tau_2}$**/ns**	4. 443	1. 89249
$\boldsymbol{\tau}$**/ns**	3.79	1.14

Calculation details of apparent quantum efficiency (AQE):

The apparent quantum efficiency (AQE) for U-1Ru/3DpCN was measured under the same photocatalytic reaction condition except for the light source. The light source was 300 W Xenon lamp equipped with a DT420 nm band-pass filter (λ = 420 ± 10 nm). The photo intensity was confirmed by Solar Power Meter (SM206), the irradiation area was controlled as 40.7 cm^2, and the photocatalytic reaction was controlled for 1 h. The AQE was calculated from equation as follows:

$$AQE = \frac{N_e}{N_p} \times 100\% = \frac{2 \times M \times N_A \times h \times c}{S \times P \times t \times \lambda} \times 100\%$$

where N_e is the amount of reaction electrons, N_p is the incident photons, M is the amount of H_2 molecule, N_A is Avogadro constant, h is the Planck constant, c is the speed of light, S is the irradiation area, P is the intensity of the irradiation, t is the photoreaction time, and λ is the wavelength of the monochromatic light.

When λ = 420 nm, P = 12.7 W $\cdot m^{-3}$, t = 1 h, H_2 production = 31 μmol,

$$N_p = \frac{S * P * t}{h * c/\lambda} = \frac{40.7 \times 10^{-4} \times 12.7 \times 3600 \times 420 \times 10^{-9}}{6.626 \times 10^{-34} \times 3 \times 10^{8}} = 3.9 \times 10^{20}$$

$$N_e = 2 * M * N_A = 2 \times 31 \times 10^{-6} \times 6.02 \times 10^{23} = 3.73 \times 10^{19}$$

$$AQE = \frac{N_e}{N_p} \times 100\% = \frac{3.73 \times 10^{19}}{3.9 \times 10^{20}} = 9.5\ \%$$

Table S3. Comparison of the catalytic activities and AQE of the co-catalysts/g-C_3N_4 photocatalytic systems.

Photocatalyst	H_2 production (μmol h^{-1} g^{-1})	AQE at 420 nm	Reference
U-1Ru/3DpCN	**2945.47**	**9.5%**	**Our work**
Ni_3C/g-C_3N_4	303.6	0.40%	1
Ni_2P/g-C_3N_4	362.4	1.8%	2
Ni-Mo/g-C_3N_4	1785	0.05%	3
NiO/g-C_3N_4	68.8	0.04%	4
MoS_2/g-C_3N_4	1350	2.1%	5
$Ni(OH)_2$/g-C_3N_4	152	1.1%	6
CoP/g-C_3N_4	1924	12.4%	7
CQD/g-C_3N_4	3538.3	10.94%	8

DFT calculations details:

We consider the reaction mechanism of the HER on the surface of g-C_3N_4 to be the same as the one in electrocatalysis because of the same active sites and electrons with high energy.[9] In alkaline solution, the HER process is mainly composed of H* intermediates formation and H_2 formation, which could be represented as: [10]

$$H_2O + e^- + g\text{-}C_3N_4 \rightarrow H^* \text{-} g\text{-}C_3N_4 + OH^- \text{ (Volmer step)}$$

$$2H^* \text{-} g\text{-}C_3N_4 \rightarrow H_2\uparrow \text{ (Tafel step)}$$

$$H^* \text{-} g\text{-}C_3N_4 + H_2O + e^- \rightarrow g\text{-}C_3N_4 + OH^- + H_2\uparrow \text{ (Heyrovsky step)}$$

In photocatalysis, the hydrogen binding energy (ΔE_{H*}) and hydrogen-adsorption Gibbs free energies (ΔG_{H*}) can be calculated as following equation:[10,11]

$$\Delta E_{H*} = E_{H*\text{-}g\text{-}C_3N_4} - E_{g\text{-}C_3N_4} - 1/2\, E_{H_2}$$

$$\Delta E_{H*} = E_{H*\text{-}x} - E_x - 1/2\, E_{H_2}$$

$$\Delta G_{H*} = \Delta E_{H*} + \Delta E_{ZPE} - T\,\Delta S$$

$E_{H*\text{-}x}$ and E_x refer to the total energies of X (X = Ru, Pt, g-C_3N_4, Ru/g-C_3N_4 and Pt/g-C_3N_4) with and without hydrogen adsorption, respectively. ΔE_{ZPE} is the difference of the zero-point energy with and without hydrogen adsorption, T is the temperature (300 K), and ΔS is the entropy change between an adsorbed hydrogen and gas-phase hydrogen at 101325 Pa.

Table S4. The ΔG_{H*} values of all the H* adsorption models.

Model	ΔG_{H*} value	H* adsorption models	ΔG_{H*} value
Ru (101)	-0.12 eV	Pt (111)	-0.10 eV
g-C_3N_4	0.33 eV	Ru (101)/g-C_3N_4	0.24 eV
Pt (111)/g-C_3N_4	0.08 eV		

References

1 K. He, J. Xie, Z. Q. Liu, N. Li, X. B. Chen, J. Hu and X. Li, *J. Mater. Chem. A*, 2018, *6*, 13110.

2 W. J. Wang, T. C. An, G. Y. Li, D. H. Xia, H. J. Zhao, J. C. Yu and P. K. Wong, *Appl. Catal. B: Environ.*, 2017, **217**, 570–580.

3 X. Han, D. Y. Xu, L. An, C. Y. Hou, Y. G. Li, Q. H. Zhang and H. Z. Wang, *Appl. Catal. B: Environ.*, 2019, **243**, 136–144.

4 J. N. Liu, Q. H. Jia, J. L. Long, X. X. Wang, Z. W. Gao and Q. Gu, *Appl. Catal. B: Environ.*, 2018, **222**, 35–43.

5 Y. D. Hou, A. B. Laursen, J. S. Zhang, G. G. Zhang, Y. S. Zhu, X. C. Wang, S. Dahl and I. Chorkendorff, Angew. Chem., 2013, **125**, 3709–3713.

6 J. G. Yu, S. H. Wang, B. Cheng, Z. Lin and F. Huang, *Catal. Sci. Technol.*, 2013, **3**, 1782–1789.

7 C. M. Li, Y. H. Du, D. P. Wang, S. M. Yin, W. G. Tu, Z. Chen, M. Kraft, G. Chen and R. Xu, *Adv. Funct. Mater.*, 2017, **27**, 1604328.

8 Y. Wang, X. Q. Liu, J. Liu, B. Han, X. Hu, F. Yang, Z. Xu, Y. Li, S. Jia and Z. Li, *Angew. Chem.*, 2018, **130**, 5867–5873.

9 Q. H. Zhu, B. C. Qiu, H. Duan, Y. T. Gong, Z. W. Qin, B. Shen, M. Y. Xing and J. L. Zhang, *Appl. Catal. B: Environ.*, 2019, **259**, 118078.

10 Y. L. Sun, D. Jin, Y. Sun, X. Meng, Y. Gao, Y. Dall′ Agnese, G. Chen and X. F. Wang, *J. Mater. Chem. A*, 2018, **6**, 9124–9131.

11 S. Y. Nong, W. J. Dong, J. W. Yin, B. W. Dong, Y. Lu, X. T. Yuan, X. Wang, K. J. Bu, M. Y. Chen, S. D. Jiang, L. M. Liu, M. L. Sui and F. Q. Huang, *J. Am. Chem. Soc.*, 2018, **140**, 5719−5727.